2022 American Control Conference (ACC)
Atlanta, USA, June 8-10, 2022

EQUIVALENT CIRCUIT MODEL FOR HIGH C-RATE DISCHARGE WITH AN EXTERNAL SHORT CIRCUIT

Vivian Tran[1*], Ting Cai[1], Anna Stefanopoulou[1], and Jason Siegel[1]

***Abstract*— To improve emergency responder safety while handling damaged battery packs after a fire, better external short-based discharge methods are needed to mitigate hazards from stranded energy, including battery fire reignitions. This work uses a linear scaling on the diffusion-related parameters of an equivalent circuit model to capture the electrical and thermal behavior of a cell during an external short for different initial state-of-charge (SOC). As metrics of discharge effectiveness and safety, the model predicts the final SOC within 3%SOC and peak temperature within 2°C in the fitted, fully charged case. The same parameter set was applied to all initial SOC cases and parameter sensitivity is discussed. A key advantage of the proposed approach is that the main parameterization can be performed under normal operating conditions reducing the amount of hazardous testing required. This can then be used to explore a controlled discharge by adjusting the external resistance to avoid venting.**

I. Introduction

The use of Li-ion batteries is expected to grow dramatically in the next decade with the forecasted growth of electric vehicles (EVs) and battery energy storage syste
In the history of EVs, evidence shows that EVs
to catch fire than conventional vehicles [1], [
battery pack and system fires can still occur
despite the engineered protections and reignite
later due to stranded energy in damaged batt
new challenges for emergency responders [3
more effective discharge methods are neede
the stranded energy and quickly discharge ba
to very low state-of-charge (SOC) where the
risk and severity of battery thermal runaway [4
field-parameterizable models that can guide th
external short-based strategies may allow us to
and control a fast discharge.

Prior modeling work for battery external
(ESC) from Mao et al. [5] used a Dualfoil mod
behavior under a small constant-resistance lo
the transport limitations, but experimental valid
done. Similarly, Rheinfeld et al. [6] used a Dualfoil model and implemented concentration-limited reaction kinetics to capture the diffusion limitations in the electrolyte and active material. Experimental validation was done with single-layer cells with a quasi-isothermal set-up, so temperature evolution was not modeled [6]. Smith et al. [7] modeled and experimentally validated an equivalent circuit model (ECM) for a 16P module of cylindrical cells with positive-temperature coefficient (PTC) devices that effectively prevented first venting and thermal runaway. In this case, the max C-rate is only about 7.5C, and the PTC devices tripped 12 seconds after the start of the short, dropping the current to C/5 [7]. However, large battery systems also use other cell formats (i.e. pouch) which do not have the same built-in safety devices and can experience higher C-rates and temperatures.

In this work, the goal is to extend a simple battery cell model from normal operating conditions to an external short condition with a maximum C-rate of 50C. The model will be used to predict discharge effectiveness, which can be quantified by final SOC, and safety risks, which can be informed by the peak temperature. This paper will first discuss the experimental setup for the external short circuit testing. Next, the electrical equivalent circuit model will be presented with a discussion on the adaptation and tuning needed to capture the bulk ESC behavior from normal operating characterization. Then, the lumped thermal model will

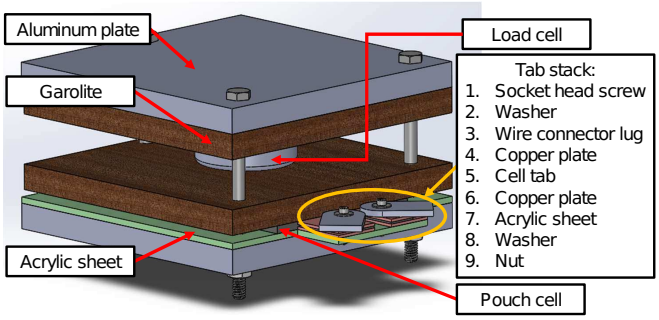

Fig. 1: External short circuit cell fixture

II. Experimental Setup

For the experiment, three NMC-graphite pouch cells with a fresh capacity of 5 Ah manufactured by the University of Michigan Battery Lab were used. The cells were calendar-aged at room temperature during storage down to 4.6 Ah at the time of the test. The cells were externally shorted with an average external resistance of about 6.8 mΩ from initial SOCs of 100, 75, and 50%.

The cell type and experimental setup are the same as what was reported in Cai et al. [8]. Two K-type thermocouples (accuracy ±2.2°C) were placed to measure the cell surface

[1] Department of Mechanical Engineering, University of Michigan, Ann Arbor, MI 48109
∗ Corresponding author: Vivian Tran (vvttran@umich.edu)

temperature at the center of the cell and near the tabs. The pouch cell was then placed between two poron sheets in a fixture instrumented with an Omegadyne LC305-500 load cell. The fixture was then placed in an acrylic box with a Telaire T6703 NDIR CO_2 sensor, all inside a fume hood. The cell tabs were reinforced and secured to the acrylic plate to ensure a reliable connection to the circuit and prevent contact between the tabs during setup and testing as seen in Fig. 1. After securing the cell, the tabs were connected to either side of an open Gigavac GV141BAB DC contactor (max contact resistance of 0.4 mΩ and insulation resistance of 100 MΩ) in series with a NUVX-LB-200-100 current shunt rated at 200 A at 100 mV (0.5 mΩ resistance with ±0.25% tolerance) using 4 AWG wires. Voltage was measured using a National Instrument SCXI-1102 module (±4 mV accuracy). The cell current, voltage, surface temperature, vent gas CO_2 concentration, and expansion force measurements were taken at 10 Hz. The short circuit was initiated by supplying a 12 V signal to the contactor to close the circuit. The electrical and thermal experimental results can be seen in Fig. 2. For the fully charged cell, the expansion force and CO_2 concentration were reported in [8].

The initial and maximum C-rate in all cases was about 50C, which is abnormally high for these energy cells, while the initial voltage dropped to about 1.5 V. SOC was calculated based on Coulomb counting. While all three cells expanded over the duration of the short circuit, only the 100% initial SOC cell vented after 80 seconds [8]. The measured maximum cell center temperatures and final SOCs are summarized in Table I, which are the metrics this model will try to predict.

TABLE I: Summary of key metrics from experimental results

SOC_0 (%)	SOC_f (%)	T_{max} (°C)
100	34.6	120.3
75	20.8	109.8
50	1.1	105.6

Since the fully charged cell represents the most hazardous case here, it was chosen as the cell to parameterize the electrical and thermal models. The same set of parameters was then applied to simulate the other initial SOC cases.

III. Electrical Model

In modeling an external short circuit for the purpose of predicting the behavior during a fast and safe cell discharge, predicting the final SOC is an important metric for evaluating effectiveness. Additionally, because future investigations will look to scale up the model to predict module- and pack-level behavior during discharge, an equivalent circuit model was chosen for its simplicity and low number of parameters.

In the ESC electrical model shown in Fig. 3, a single RC equivalent circuit is used. The constant tabbing series resistance term, R_{tab}, is included to account for additional contact resistance at the connection between the clips used for voltage measurement and the tab reinforcement stack. Therefore, the measured terminal voltage, V_t, includes the nominal single RC and the voltage drop across R_{tab}.

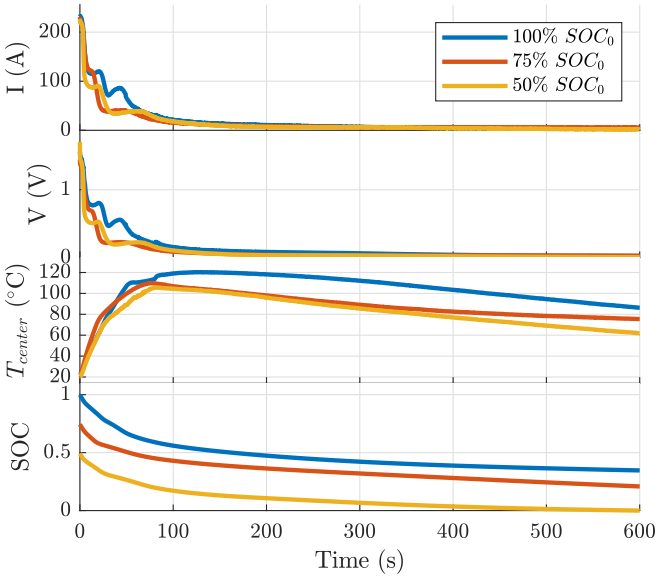

Fig. 2: Experimental data for a ten-minute ESC. From top to bottom, these are measured ESC current, voltage, center temperature, and calculated SOC.

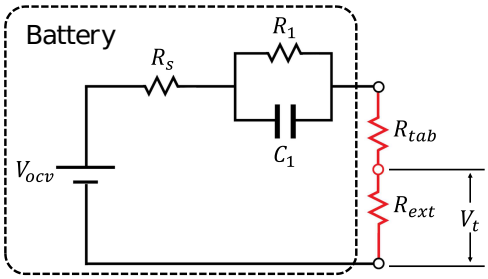

Fig. 3: Battery equivalent circuit model with a single RC pair and additional series R_{tab}.

A. Nominal single RC model

The electrical behavior for the cell is described by two ordinary differential equations for the SOC and capacitor voltage, V_1,

$$\begin{bmatrix} \dot{SOC} \\ \dot{V_1} \end{bmatrix} = \begin{bmatrix} 0 & 0 \\ 0 & -\frac{1}{R_1 C_1} \end{bmatrix} \begin{bmatrix} SOC \\ V_1 \end{bmatrix} + \begin{bmatrix} -\frac{1}{Q} \\ \frac{1}{C_1} \end{bmatrix} I(t) \quad (1)$$

$$V_t(t) = V_{ocv}(SOC) - V_1 - (R_s + R_{tab})I(t) \quad (2)$$

where R_s, R_1, and C_1 are SOC-dependent parameters, and Q is the capacity of the cell calculated from a 1C constant-current, constant-voltage (CCCV) discharge. $V_t(t)$ and $V_{ocv}(SOC)$ are the terminal voltage and open-circuit voltage, respectively. $I(t)$ is the short circuit current, where $I > 0$ for discharge, and is calculated as

$$I(t) = \frac{V_{ocv} - V_1}{R_{ext} + R_{tab} + R_s}. \quad (3)$$

Physically, the voltage drop across R_s can be interpreted as the internal cell resistance, e.g. contact resistances. The voltage across the RC pair, V_1, can be interpreted as a voltage polarization due lithium diffusion in the solid and electrolyte. For the system, the time constant is defined as $\tau = R_1 C_1$.

For the nominal model parameterization, 2C pulse characterization testing of the 100% initial SOC cell was done at room temperature by alternating 2 min pulses at 2C (9A) and 5 min rests (Fig. 4a). The R_s, R_1, and C_1 parameters were obtained through an auto-regressive, least-squares fitting of the data at each pulse (Fig. 4b). The model was validated with a voltage root mean square error (RMSE) of 0.029 V, which is comparable to other ECMs [9].

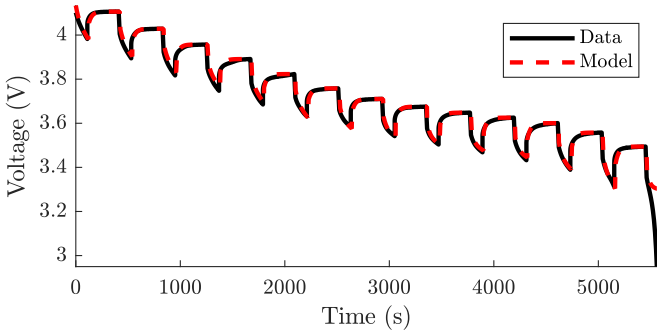

(a)

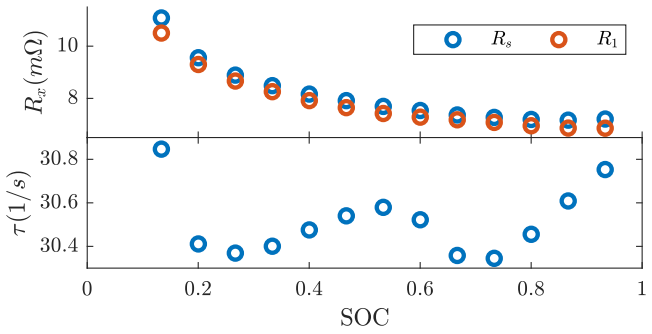

(b)

Fig. 4: 2C pulse test characterization (a) nominal electrical model validation and (b) ECM parameters.

B. Tab and external circuit resistances

Due to the additional resistance expected from the voltage leads connected to the tab reinforcement stack and cell tabs during the experimental setup, the measured voltage and current are used to identify a tab resistance. R_{tab} in the model was evaluated as the difference between the resistance calculated from the measured initial voltage drop ($V_{t,0}$) and measured initial current (I_0), and expected initial $R_s(SOC_0)$, where SOC_0 is the initial SOC. The external resistance, R_{ext}, was calculated with Ohm's law as the initial voltage after the voltage drop divided by the initial current.

$$R_{tab} = \frac{1}{I_0}(V_{OCV}(SOC_0) - V_{t,0}) - R_s(SOC_0) \quad (4)$$

$$R_{ext} = \frac{V_{t,0}}{I_0} \quad (5)$$

After further analysis, the main metrics of interest (e.g. peak temperature and final SOC), were not sensitive to a 10% change in these parameters in the simulations, so the set of R_{ext} and R_{tab} obtained for the 100% initial SOC cell was also used in the other initial SOC simulations.

C. Scaling of the nominal RC parameter functions

At abnormally high temperatures and C-rates observed in an external short, two competing factors affect diffusion, namely improved reaction kinetics and mass transport limitations, respectively. Looking at other works that model more normal operating conditions, Arrhenius parameter dependencies are used to capture increased reaction kinetics at higher temperatures, which correspond to a decrease in R_1 and increase in C_1 [7], [9]. However, under external short conditions, the cell discharge behavior is dominated by mass transport limitations in electrolyte and solid diffusion from operating at high currents [5], [10].

To capture the measured current and voltage decay from the external short circuit, the time constant, R_1C_1, needs to be increased. A linear scaling of the diffusion-related parameters was chosen due to the simplicity of the modification and its ability to represent the overall effect. The entire R_1 and C_1 curves are scaled by constants α and β, respectively, where $R_1(SOC)$ and $C_1(SOC)$ are the curves used in the ESC model and $\tilde{R}_1(SOC)$ and $\tilde{C}_1(SOC)$ are the original parameters from pulse test characterization

$$R_1 = \alpha\tilde{R}_1(SOC) \quad (6)$$

$$C_1 = \beta\tilde{C}_1(SOC). \quad (7)$$

The parameterization for α and β is formulated as a constrained optimization problem (Eq. 8). The objective function is designed to reflect the goals of the model, which are to predict the final SOC and peak temperature. Therefore, penalties for SOC and cell temperature errors are included in addition to current.

$$\begin{aligned} \underset{\alpha,\beta}{\text{argmin}} \quad & J = \frac{||\hat{I} - I||_2}{I_{max}} + \frac{||S\hat{O}C - SOC||_2}{\Delta SOC} + \frac{||\hat{T} - T||_2}{\Delta T} \\ \text{subject to} \quad & 10 < \alpha < 250 \\ & 0.1 < \beta < 1 \end{aligned} \quad (8)$$

where $\hat{I}$, $S\hat{O}C$, and $\hat{T}$ are the simulated current, SOC, and cell temperature, respectively. The thermal model and parameterization will be presented in the following section. From the data, I_{max} is the maximum measured current, ΔSOC is the total change in SOC during discharge ($SOC_{max} - SOC_{min}$), and ΔT is the total change in measured cell center temperature ($T_{max} - T_{min}$). For the ten-minute ESC of the 100% SOC_0 cell, these are 232 A, 0.65 (65%SOC), and 96 K, respectively. The optimization problem was solved used the MATLAB functions `multistart` with 20 local solvers and `fmincon` with the interior-point algorithm and an optimality tolerance of 1e-6.

The bounds on α and β were chosen based on a grid search guided by a set of manually tuned parameters where α=100 and β=0.5. For the grid search, the ESC was simulated with $\alpha \in [10, 1000]$ and $\beta \in [0.05, 50]$ for the objective function J (Eqn. 8). The parameter sweep identified a region near the minimum within the search space that was used to refine the bounds on α and β for faster optimization convergence; however, the bounds are ultimately arbitrary.

The sweep suggested that the problem is locally convex, but more analysis is needed to prove this.

For the fully charged cell, α and β were fitted to be 64.53 and 0.48, respectively, ultimately increasing the time constant by a factor of 31. These same values were then applied to the 75% and 50% initial SOC cases as well. A summary of the electrical parameters used in the subsequent simulations are provided in Table II.

TABLE II: Summary of electrical model parameters

Parameter	Value	Unit	Description	Source
Q	4.6	Ah	Cell capacity	Measured
R_{ext}	6.7	$m\Omega$	External resistance	Calculated
R_{tab}	4.1	$m\Omega$	Tabbing resistance	Calculated
α	64.53	-	$R_1(SOC)$ scalar	Fitted
β	0.48	-	$C_1(SOC)$ scalar	Fitted

D. Electrical model results

ESCs were simulated for each initial SOC condition. The simulation results compared to data can be seen in Figure 5. Errors for measured values z are calculated as $e_z = \hat{z} - z$, where $\hat{z}$ is the predicted value. In application, the initial SOC may not be known or measurable; however, the results show that across relatively high initial SOCs, the same parameter set and linear scalings on the diffusion-related parameters work well in predicting the final SOC after a ten-minute short circuit as seen in Table III. For the ten-minute ESC of the fully charged cell, the model captures the intermediate current decay from a peak of 232 A down to below 3 A and similarly for the voltage decay from 1.6 V to 25 mV. The RMSEs for current and voltage are 24.09 A and 0.16 V, respectively. During the first two minutes, the absolute SOC error peaks due to the error in the predicted current, but decreases and ultimately underpredicts the final SOC by less than -3%SOC (5% of ΔSOC).

Applying the same parameters to the 75% and 50% SOC_0 cells, maximum final SOC error is in the 75% SOC_0 case which was underpredicted by -6.5%SOC (12% of ΔSOC) to be 14.3%SOC whereas the calculated SOC from the measured current is 20.8%SOC. Additional error metrics are provided in Table III.

TABLE III: Final SOC error and RMSE of current, voltage, and SOC

SOC_0 (%)	e_{SOC_f} (%)	RMSE I (A)	RMSE V (V)	RMSE SOC (%)
100	-2.9	24.09	0.16	2.4
75	-6.5	28.34	0.24	6.8
50	0.4	28.43	0.23	3.7

Because of the simplicity of the model, not all of the dynamics can be captured, especially during the first minute of the short circuit. The step-wise current and voltage behavior during the first minute of discharge can be attributed to high-current, mass transport limitations [10]. This is due to local Li depletion in the electrolyte and particle surface at very high currents, which can be modeled with a detailed

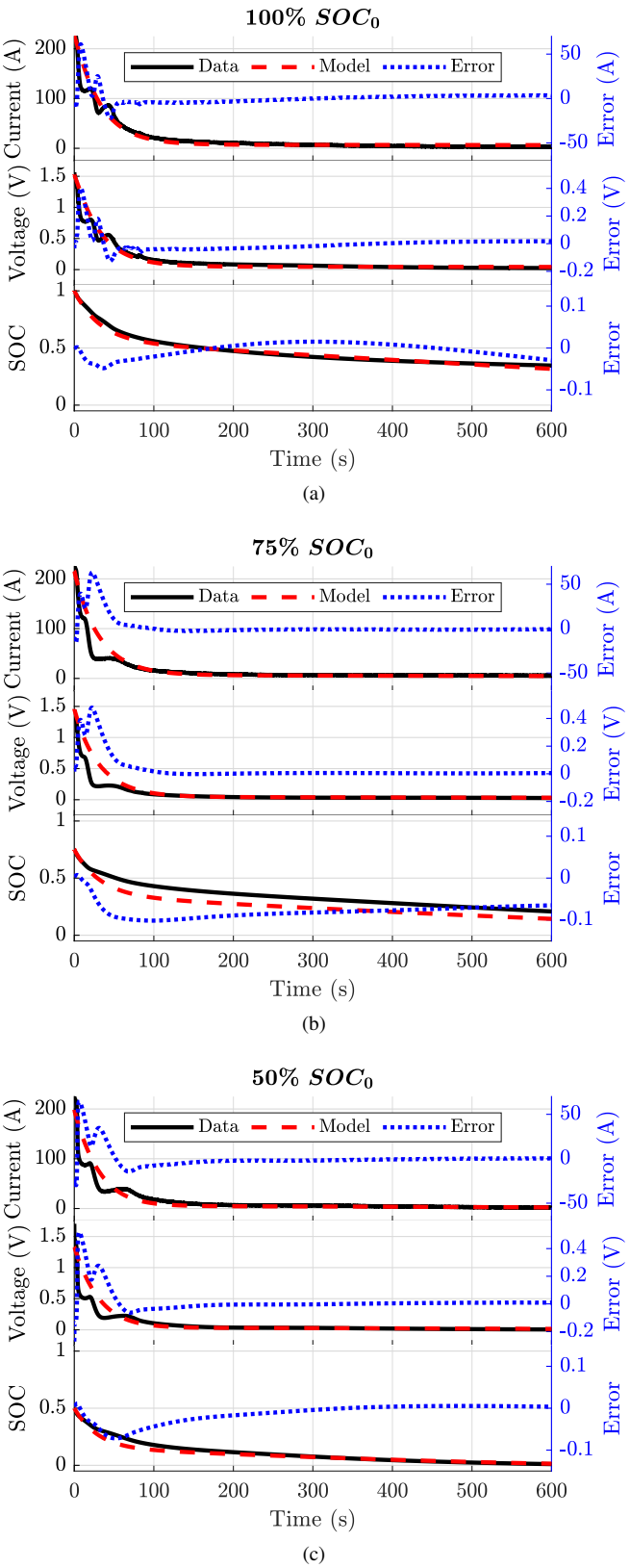

Fig. 5: Comparison of ESC experimental data and electrical model results for a) 100%, b) 75%, and c) 50% initial SOC.

electrochemical model, such as the Dualfoil model [6]. However, a single RC equivalent circuit model does not have the mechanisms to describe this. Still, the error in the predicted SOC after ten minutes across all three cases is at most 6.5%SOC. Recall that the current shunt has an accuracy of 0.25% full-scale range, so over the duration of the ESC, measurement error can account for up to 1.8%SOC in the final SOC. Keeping in mind the limitations, we proceed to use the electrical model to predict the cell thermal behavior.

IV. Thermal Model

For discharging compromised cells, modeling and predicting the peak temperature is also important to help evaluate safety risks. The thermal model is a lumped thermal model with the total heat generation modeled as the sum of the Ohmic heating terms from the R_{tab}, R_s, and RC pair

$$Q_{ohmic} = I(V_t - V_{OCV}) = I^2(R_{tab} + R_s) + IV_1. \quad (9)$$

The cell within the fixture is modeled as a single thermal mass with heat dissipated through convection. The cell temperature is described by

$$\begin{aligned} \frac{dT}{dt} &= \gamma Q_{ohmic} - \eta(T - T_{amb}) \\ \gamma = \frac{1}{m_{cell}C_p}, &\quad \eta = \frac{-Ah}{m_{cell}C_p} \end{aligned} \quad (10)$$

where m_{cell} is the mass of the cell, C_p is the effective heat capacity of the cell, and h is the effective convective heat transfer coefficient.

A. Thermal parameterization of h and C_p

Because the cell is in a fixture that provides additional thermal mass and cooling area with additional insulation provided by thin poron sheets, h and C_p are considered to be effective parameters. These are found using a similar formulation to Kim et al. [11], neglecting reversible heating. For the parameterization, the Ohmic heat generation is calculated using Eq. 9 with measured current and voltage. Although the fully charged cell vented during the experiment, the solid-electrolyte interphase (SEI) decomposition heating is assumed to be negligible compared to the Ohmic heat [12]. An unconstrained optimization problem is formulated as

$$\underset{\eta,\gamma}{\text{argmin}} \quad J = ||\hat{T}(\eta,\gamma) - T||_2. \quad (11)$$

where $\hat{T}$ is the simulated cell temperature, and T is the measured cell center temperature. The parameters γ and η are found from solving the optimization problem and are used to calculate h and C_p. These were initialized using A from [8] and m_{cell} from [13], which are previous studies that use the same type of cell, with a $C_{p,0}$ of 1200 $\frac{J}{kg.K}$ and h_0 of 5 $\frac{W}{K.m^2}$. The optimization problem was solved used the MATLAB function `fminunc` with the quasi-Newton algorithm and an optimality tolerance of 1e-6. The final C_p and h used in the model are 2108 $\frac{J}{kg.K}$ and 54.06 $\frac{W}{K.m^2}$, respectively. For the external short of the fully charged cell, thermal model validation with measured current and voltage input can be seen in Figure 6, where the RMSE is 1.96°C. Table IV summarizes the thermal model parameters.

TABLE IV: Summary of thermal model parameters

Parameter	Value	Unit	Description	Source
m_{cell}	104	g	Cell mass	[13]
A	0.009	m^2	Cell cooling area	[8]
h	54.06	$\frac{W}{K.m^2}$	Eff. convective heat transfer coeff.	Fitted
C_p	2108	$\frac{J}{kg.K}$	Eff. cell heat capacity	Fitted
T_{amb}	293.8	K	Ambient temperature	Measured

B. Thermal model results

Looking at the predicted temperature profile, across all initial SOC cases the thermal model underpredicted the maximum change in temperature by almost -2°C (2% of ΔT) in the 100% initial SOC case and as much as -15°C (18% of ΔT) in the 50% initial SOC case.

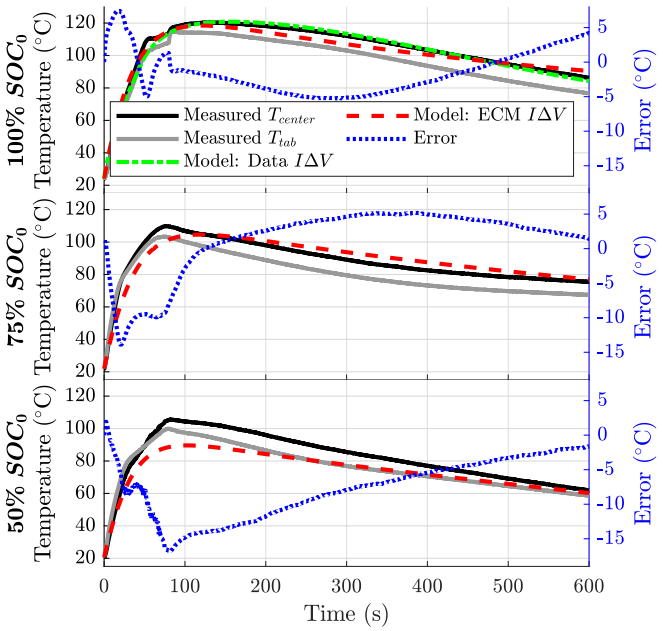

Fig. 6: Measured cell center and tab temperatures and model results. Error is calculated between the thermal model with modeled Q_{Ohmic} and measured center temperature.

TABLE V: Maximum error and RMSE for cell temperature

SOC_0 (%)	$e_{T_{max}}$ (°C)	RMSE T (°C)
100	-1.81	4.30
75	-5.25	8.32
50	-15.96	7.81

Looking at the contributions of the individual heat sources from the fully charged case before venting ($t \leq 80$s), Ohmic heating from R_s, R_{tab}, and V_1 account for 60%, 34%, and 6%, respectively. The dominant sources of heat generation are Ohmic heating from the series resistances, which can be identified under normal operating conditions. This also emphasizes the importance of reducing the error in the modeled current since these terms are $Q_{ohmic,R} \propto I^2$. This can be seen with decreasing SOC_0 where $RMSE\ I$ (Table III) increases along with $RMSE\ T$ and $|e_{T_{max}}|$ (Table V).

V. Parameter sensitivity

Looking at the parameter sensitivity for the 100% initial SOC case, for a ±10% change in individual electrical parameters, R_{ext} and R_{tab} had a small effect on the final SOC ($\leq \pm 1$%SOC), but R_{ext} had a moderate effect on the change in temperature (±2 °C). For a ten-minute discharge, a 10% change in the scalars of R_1 and C_1 changed the final SOC by about ±2%SOC and ±3.5%SOC, respectively. However, β, the scalar on C_1, had a relatively large effect on the change in temperature (±6 °C), while α, the scalar on R_1, had a smaller effect on the change in temperature ($\leq \pm 1$ °C). In general, the two main metrics of final SOC and peak temperature were most sensitive to the scalar β on C_1.

TABLE VI: Change in model error for ±10% parameter change for the 100% initial SOC cell

Electrical Parameter	Percent change	Parameter value	Error - Nominal Error	
			Final SOC (%)	ΔT (°C)
R_{ext} (mΩ)	+10%	7.4	0.1	-1.9
	-10%	6.1	-0.1	2.0
R_{tab} (mΩ)	+10%	4.5	0.1	0.3
	-10%	3.7	-0.1	-0.3
α in (6)	+10%	70.98	1.8	-0.5
	-10%	58.07	-2.2	0.6
β in (6)	+10%	0.53	-3.4	6.2
	-10%	0.43	3.5	-6.4
hA	+10%	0.54	-	-1.7
	-10%	0.48	-	1.9
mC_p	+10%	241	-	-7.3
	-10%	197	-	8.9

Similarly, in the thermal model, a ±10% change in hA has a moderate effect and changed the maximum cell temperature by almost 2°C, while changing mC_p has a large effect on the final temperature changing the overall ΔT by between 7-9°C. Because the RC parameters are not temperature dependent, there is no effect on the final SOC.

VI. Conclusion

Modeling external short circuits can help build an understanding of the potential efficacy of leveraging ESC-based strategies and shorting media for discharging stranded energy in a battery system. Towards this goal, this work looked at how to extend an equivalent circuit model with parameters extracted from characterization testing within normal operating limits to capture the bulk external short circuit current and voltage behavior. This was coupled with a lumped thermal model to capture the peak temperature. As a first attempt, this does reasonably well in capturing the final SOC across a wide range of higher SOCs ($\leq$6.5%SOC error) and peak temperature for cells at 100% and 75% SOC_0. To more accurately capture the entire temperature profile including the magnitude and timing of the peak temperature, greater accuracy in the modeled current may be needed, e.g. including C-rate dependency on the diffusion-related parameters and modeling the current-step behavior during mass transport limited discharge. As future work, a venting model can be coupled to the presented model to predict venting timing and better evaluate additional safety hazards associated with the release of flammable gases and ejecta. When combined, a model predictive control approach can be used to define an optimal resistance profile based on pressure and temperature constraints to avoid venting. In context, these efforts ultimately hope to help guide the design of improved ESC-based discharge strategies to ensure that emergency responders are prepared for the rapidly changing and increasingly electrified landscape.

Acknowledgement

The authors would like to thank the National Science Foundation under Grant No. 1762247 and the UM Energy Institute providing funding to support the project. The authors would like to thank the UM Battery Lab for their help with the battery abuse experiments, and Dale Igram (UM) for his help with the background research.

References

[1] Price, Jane and Cheung, Ivan, "Safety risks to emergency responders from lithium-ion battery fires in electric vehicles: Prevalence of electric vehicle battery fires," NTSB, Tech. Rep., 2018.

[2] Tesla Inc, "Tesla vehicle safety report," Apr 2021.

[3] NTSB, "Safety risks to emergency responders from lithium-ion battery fires in electric vehicles," NTSB, Tech. Rep., 2020.

[4] X. Feng, S. Zheng, D. Ren, X. He *et al.*, "Investigating the thermal runaway mechanisms of lithium-ion batteries based on thermal analysis database," *Applied Energy*, vol. 246, pp. 53–64, 2019.

[5] J. Mao, W. Tiedemann, and J. Newman, "Simulation of li-ion cells by dualfoil model under constant-resistance load," *ECS Transactions*, vol. 58, no. 48, p. 71, 2014.

[6] A. Rheinfeld *et al.*, "Quasi-isothermal external short circuit tests applied to lithium-ion cells: Part ii. modeling and simulation," *Journal of The Electrochemical Society*, vol. 166, no. 2, p. A151, 2019.

[7] K. Smith, G.-H. Kim, E. Darcy, and A. Pesaran, "Thermal/electrical modeling for abuse-tolerant design of lithium ion modules," *International Journal of Energy Research*, vol. 34, no. 2, pp. 204–215, 2010.

[8] T. Cai, V. Tran, J. Siegel, and A. Stefanopoulou, "Modeling li-ion battery first venting events before thermal runaway," in *Proc. of the 1st Modeling, Estimation and Control Conference 2021*, 2021.

[9] X. Lin, H. E. Perez, S. Mohan, J. B. Siegel *et al.*, "A lumped-parameter electro-thermal model for cylindrical batteries," *Journal of Power Sources*, vol. 257, pp. 1–11, 2014.

[10] A. Kriston, A. Pfrang, H. Döring, B. Fritsch *et al.*, "External short circuit performance of graphite-lini1/3co1/3mn1/3o2 and graphite-lini0. 8co0. 15al0. 05o2 cells at different external resistances," *Journal of Power Sources*, vol. 361, pp. 170–181, 2017.

[11] Y. Kim, S. Mohan, J. B. Siegel, and A. G. Stefanopoulou, "Maximum power estimation of lithium-ion batteries accounting for thermal and electrical constraints," in *Dynamic Systems and Control Conference*, vol. 56130. ASME, 2013, p. V002T23A003.

[12] P. T. Coman, E. C. Darcy, C. T. Veje, and R. E. White, "Modelling li-ion cell thermal runaway triggered by an internal short circuit device using an efficiency factor and arrhenius formulations," *Journal of The Electrochemical Society*, vol. 164, no. 4, pp. A587–A593, 2017.

[13] T. Cai, A. G. Stefanopoulou, and J. B. Siegel, "Modeling li-ion battery temperature and expansion force during the early stages of thermal runaway triggered by internal shorts," *Journal of The Electrochemical Society*, vol. 166, no. 12, p. A2431, 2019.